Department of Aeronautics, Imperial College London

AERO97051 Applied Computational Aerodynamics

Coursework Assignment 2020-21

Name	XERXES CHONG XIAN	CID No	01389744

Part A: 2D Aerofoil

XFOIL

1. Common flow features (4%)

a. At what location on the upper surface is the pressure gradient adverse?

The pressure gradient is adverse at the chord-wise location of $0.05 < \frac{x}{c} < 0.06$. The pressure gradient is adverse ($\frac{dp}{dx} > 0$) due viscosity and the no-slip condition along the wall, which slows the flow and hence affects an increasing pressure downstream.

b. What are the differences in the C_p distribution between the viscous and inviscid solutions? Where are they located? What do the differences indicate? (125 words max.)

The difference is noticeable on the upper surface of the aerofoil, at $0.55 < \frac{x}{c} < 0.85$, the viscid C_p remains constant as $\frac{x}{c}$ increases before subsequently dropping. This indicates flow separation has occurred and the flow has detached from the aerofoil surface and pressure stops increasing. The eventual decrease in pressure indicates reattachment. This effect changes the effect shape of the boundary layer. As lift is the area bounded by the C_p graph, the inviscid solution corresponds to a larger value of lift. Near the trailing edge at approximately $\frac{x}{c} > 0.90$, the inviscid solution recovers to a higher value of C_p as compared to the viscid solution. This indicates that there were more energy losses in the viscid solution because of viscosity.

2. Description of relevant flow phenomena at Re = 10^5 (15%)

a. Is there flow separation and/or reattachment? Is there a separation bubble? If so, mention where each phenomena is/spans based on the relevant features you can distinguish from the indicators (C_p, C_f, $\delta*$ and θ plots). How does each observed phenomena affect the relevant indicator? (250 words max.)

Flow separation and attachment has occurred with a separation bubble present on the upper surface of the aerofoil, at $0.55 < \frac{x}{c} < 0.85$. This location coincides with a region of negative C_f. This indicates friction is acting the opposite direction; hence the flow has now reversed. This effect is corroborated by a rapid increase in δ^* on the top surface, corresponding to a decrease in $\frac{U}{U_e}$ and relatively constant C_P. δ^* and θ are the displacement and momentum thickness respectively, arising from the viscous boundary layer imposing a mass and momentum "deficit" near the wall as compared to an otherwise inviscid flow. The smaller the velocity gradients, (i.e., when more of the flow above the wall is slowed down) the larger the mass deficits and hence the larger the increase in δ^*. For a separated flow, the flow has reversed, resulting in the spike for δ^*. Re-attachment occurs at $\frac{x}{c} > 0.80$ as C_f turns positive and prior which δ^* has decreased in value as the mass flow deficit has decreased. However, θ spikes at reattachment, signalling a jump in momentum losses. Transition to a turbulent boundary layer has most likely occurred, with the turbulent stresses now also contributing to the momentum losses, on top of viscous stresses. After reattachment, C_P continues to fall as the flow encounters the adverse pressure gradient, its velocity slows down causing $\delta^*$and θ to continue increasing.

b. Is there transition to turbulence? If so, discuss its effect on the relevant indicators and state the transition location. (75 words max.)

Yes, transition takes place for $\frac{x}{c} > 0.80$, at the reattachment point of the flow to the aerofoil. δ^* decreases due to the boundary layer turning turbulent and approximating a uniform flow profile in a near wall, decreasing the mass flow deficit. C_f turns positive and C_p is at its steepest gradient, indicating a high adverse pressure gradient. θ jumps, indicating larger losses of momentum in the flow due to the addition of turbulent stresses.

3. Aerofoil performance for Re = 300 900 and XFOIL prediction (12%)

a. Write down the following parameters from the *XFOIL* simulation and experimental data:

i. $dC_l/d\alpha|_{Xfoil} = 0.092/°$; $dC_l/d\alpha|_{exp} = 0.086/°$

ii. $C_{l0}|_{Xfoil} = 0.28$; $C_{l0}|_{exp} = 0.16$

iii. $\alpha_0|_{Xfoil} = -2.50°$; $\alpha_0|_{exp} = -1.75°$

iv. $(L/D)_{max}|_{Xfoil} = 72.07$; $(L/D)_{max}|_{exp} = 53.81$

b. Comment on the scope and accuracy of *XFOIL*'s prediction ability. (150 words max.)

XFOIL has good agreement with experimental data on the lift curve slope. This indicates that the relationship between lift and angle of attack is fairly accurate within the linear regime with XFOIL. However, for the range of angles of attack, XFOIL overpredicts the lift and underpredicts the drag. This is attributed to XFOIL being unable to model the 3D effects of flow over a finite wing which are detrimental to lift production (a decrease in the effective angle of attack). At higher angles of attack, XFOIL is unable to model the complex boundary layer interactions and hence drag begins to be underpredicted. This causes the increasing discrepancy in L/D ratios seen from $-4^\circ < \frac{x}{c} < 4^\circ$. The laminar separation bubble is a problem that causes degradation of performance at low Reynolds Numbers tested. XFOIL is not able to model these effects well.

4. Plots (8%)

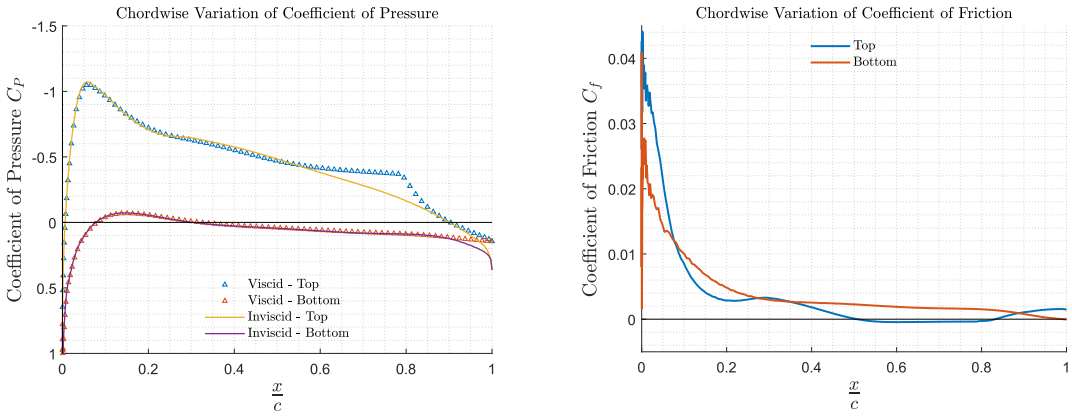

Figure 1: Variation of C_P along the chord for $Re = 10^5$ in viscous and inviscid mode (left)
Variation of C_f along the chord for $Re = 10^5$ in viscous mode (right)

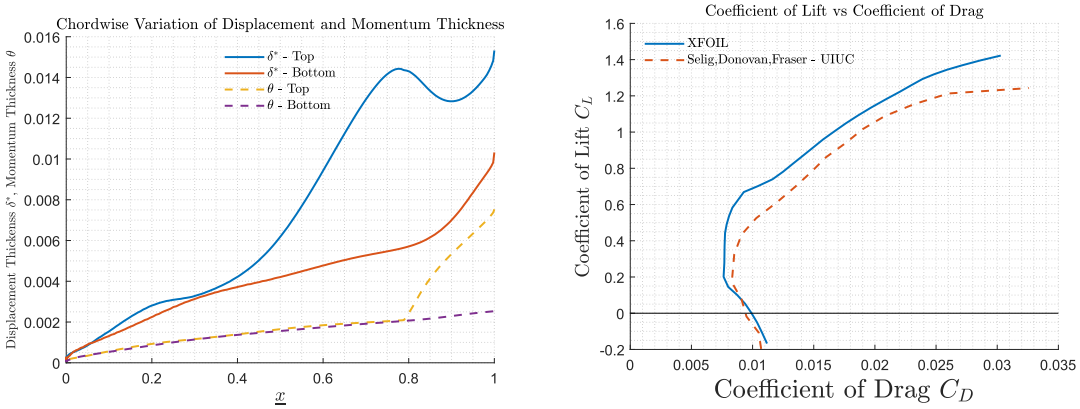

Figure 2: Variation of δ^* and θ along the chord for $Re = 10^5$ in viscous and inviscid mode (left).
C_L vs C_D at $Re = 300\,900$ for $-4^\circ \leq \alpha \leq 13.5^\circ$ (right)

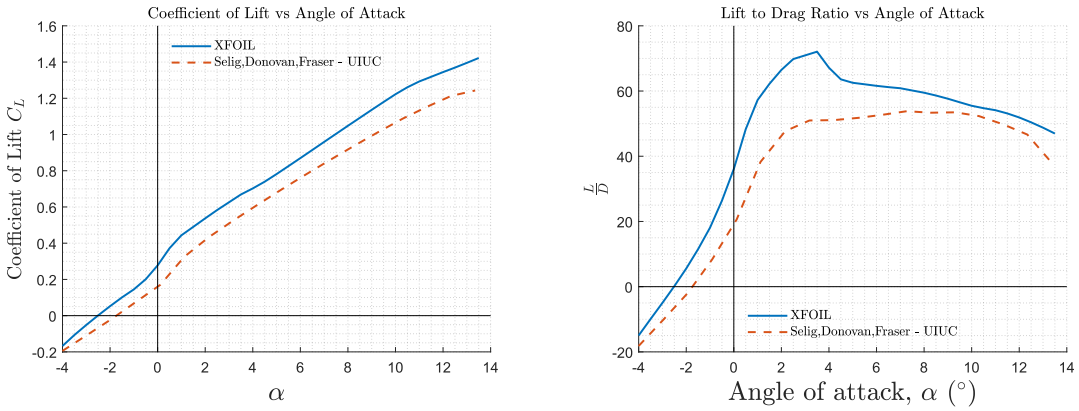

Figure 3: C_L vs α at $Re = 300\,900$ for $-4^\circ \leq \alpha \leq 13.5^\circ$ (left)
L/D vs α at $Re = 300\,900$ for $-4^\circ \leq \alpha \leq 13.5^\circ$ (right)

2D *STAR-CCM+*

1. Mesh Refinement Study (15%)

a. What prism layer count, boundary layer thickness and first prism layer thickness did you use? How did you arrive at these values? (250 words max.)

The height of the boundary layer must be first be estimated from the Equation 1:

$$\delta = \frac{0.37x}{Re_x^{1/5}}; \qquad y+ = \frac{\Delta s\, u_\tau}{\nu} \qquad (1)$$

This will be the total height of the prism layers. It is crucial that boundary layer is encapsulated by the prism layers. This requires wall y+ <1. The wall y+ value is related to the distance of the centroid of the first cell, Δs to the boundary, by the equation above, where u_τ and ν are the shear stress velocity and kinematic viscosity respectively. The following two equations were then used to find u_τ and by constraining y+<1, obtain a value for Δs. As this is the centroid position, the thickness of the first prism cell will be $2\Delta s$.

$$C_f = (2\,log(Re) - 0.65)^{-2.3}; \qquad \tau_\omega = \frac{1}{2} C_f\, \rho {U_\infty}^2 \qquad (2)$$

$$Number\ of\ Prism\ Layers = \frac{log\left(\frac{\delta}{2\Delta s}\right)}{log(Expansion\ Ratio)} \qquad (3)$$

The number prism layers were found the equation above. A suitable expansion ratio was chosen as 1.3 for aerofoil simulations. The right expansion ratio allows the prism layers to grow from the wall to meet the volume mesh smoothly (without sharp jumps in geometry from prism cell to volume cell). This reduces the chances of poor mesh quality. Although an adjusted $2\Delta s$ was obtained, the decision was made to not recalculate the number of prism layers required as doing so would have exceeded the limits set on the total cell count. $2\Delta s_{adjusted}$ still provided a smooth transition from prism layer to volume mesh hence it was deemed to be acceptable.

Table 1: Prism Layer Parameters for DF102-PT 2D simulation

Reynolds Number	300 900
Boundary Thickness, δ	0.030m
First Cell Thickness, $2\Delta s$	$5.95 \times 10^{-5}\ m$
Prism Layers	32

b. Provide the two plots for the mesh refinement study of the Cp, and the lift and drag coefficients[1]

1. This mesh refinement was accidentally performed with an additional wake refinement setting turned on. The prism layer settings were as discussed in Question 1 of this subsection. Under the advice of Professor Peiro, the simulation was not re-meshed in the interest of time. The wake refinement setting was only present in the mesh refinement section and turned off during the angle of attack study, in Question 2 of the subsection.

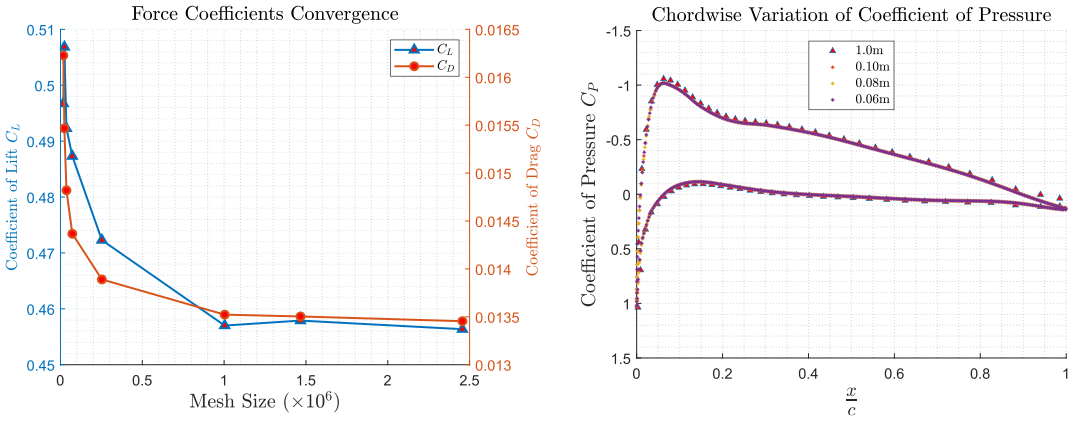

Figure 4: Convergence of C_L and C_D with increasing mesh size by varying base size (left)
Convergence of chordwise variation of C_P with increasing mesh size by varying base size (right)

c. Do the results improve? Do you see convergence? Based on your results, what base size would you select to use for further work and why? (125 words max.)

Table 2: Base sizes tested in mesh refinement and their corresponding cell count

Base Size (m)	1.00	0.80	0.60	0.40	0.20	0.10	0.08	0.06
Cells ($\times 10^6$)	0.017	0.024	0.037	0.072	0.25	1.00	1.47	2.46

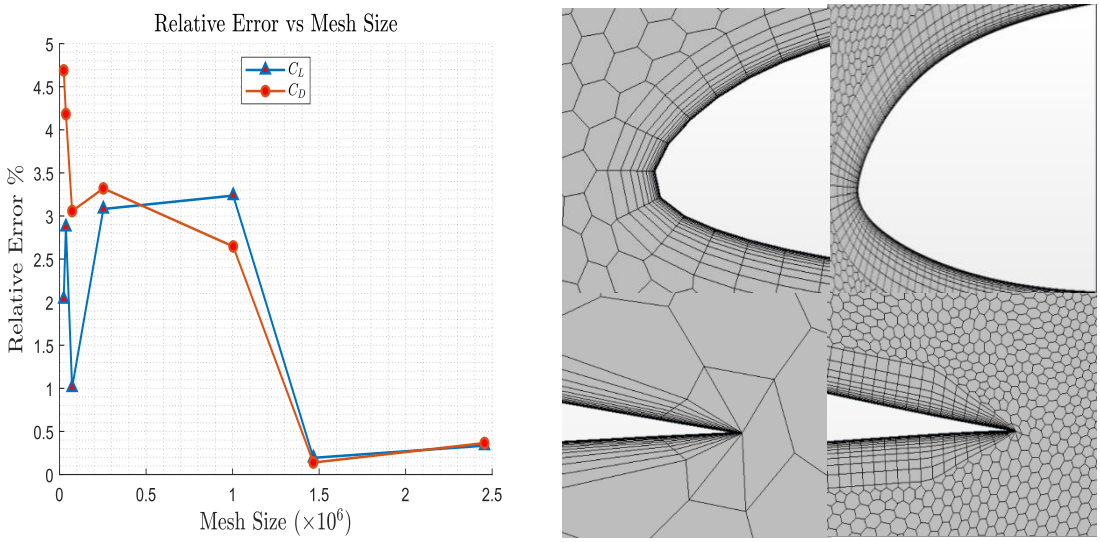

Figure 5: Relative error between integral coefficients measured between each base size (left)
Leading edge mesh at base size = 1.0m and 0.10m respectively (right, top row)
Trailing edge mesh at base size = 1.0m and 0.10m respectively (right, bottom row)

The results improve as integral values drop and tapers off at 10^6 cells. The C_P plot converges to the identical smaller "shape" as the mesh size decreases. For clarity, base sizes from 0.80m to 0.20m were not plotted. Below a base size of 0.1m, the variation is no longer significant. This also explains why the lift coefficient decreases before tapering off, as it is the closed integral of the pressure coefficient along the chord. The relative percentage error formula between the integral values obtained at each mesh size is below:

$$Relative\ Error\ ,\% = \frac{C_{Previous} - C_{Current}}{C_{Previous}} \times 100\%$$

0.1m can be taken moving forward as the error between this and the next mesh is less than 0.25% This is deemed acceptable as finer meshes add computational time with little gain in accuracy.

2. Simulation and Results (20%)

a. Provide the convergence history of the lift/drag coefficients and the residuals monitor and write down the converged coefficient values:

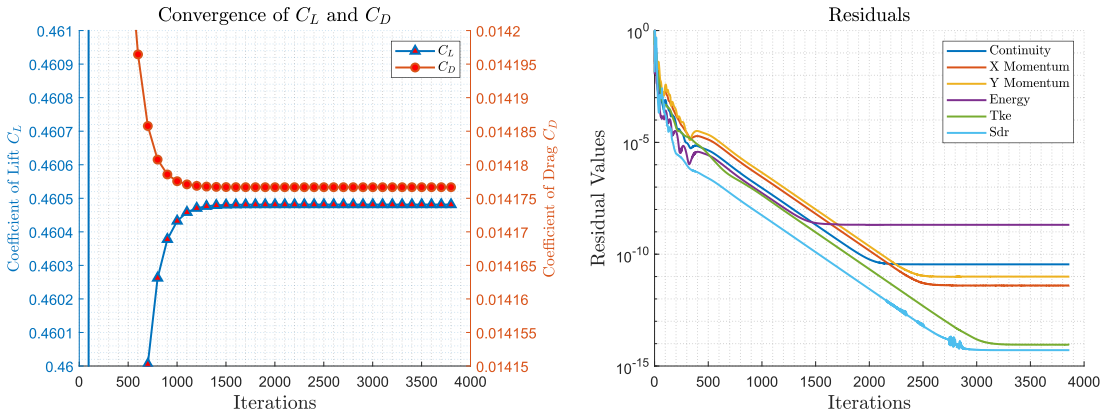

Figure 6: Convergence of integral coefficients (left) and residual values for DF102-PT simulated at $Re = 300\,900$, M = 0.3 and $\alpha = 2^{\circ}$ (right)

i. $C_L = 0.461$ ii. $C_D = 0.014$

b. What are the criteria you have used to assess convergence? (75 words max.)

i. The residuals have all dropped at least 6 orders of magnitude lower from their initial values and/or reached an asymptotic minimum.
ii. Integral coefficients fluctuate in the 5th decimal place. Since experimental data is provided up to the 4th decimal place, this is deemed as good enough.
iii. $y+_{max}$ is below 1.0 and does not fluctuate.
iv. Sensible velocity and pressure distributions from aerofoil which diminish towards the far field.

c. Briefly comment on the suitability of using a single mesh for multiple incident angles. Would the y+ target still be satisfied at different incidences? (125 words max.)

Table 3: Variation in $y+_{max}$ with α

α (°)	0.0	**2.0**	4.0	6.0	8.0	9.0	11.0	15.0
$y+_{max}$	1.07	**0.92**	1.16	1.46	1.68	1.78	1.90	1.64

A single mesh is not suitable for multiple incident angles. A change in $y+_{max}$ values was observed at different angles of attack from Table 3. The increase in angle of attack results in a larger streamline curvature at the leading edge of the aerofoil, this increases the peak velocities and local Reynolds Number and hence wall shear stress, τ_{ω}. This increases friction velocity u_{τ} and by the calculation performed in Question 1 of the 2D STAR-CCM+ study, a smaller first cell size is needed to continuously satisfy the $y+_{max} < 1$. With a constant near wall thickness for the prism layer, this observation of an increasing $y+_{max}$ with angle of attack is expected.

d. What happens when you try to simulate a high incidence flow (9 degree or higher angle of attack), why do you think this happens? (125 words max.)

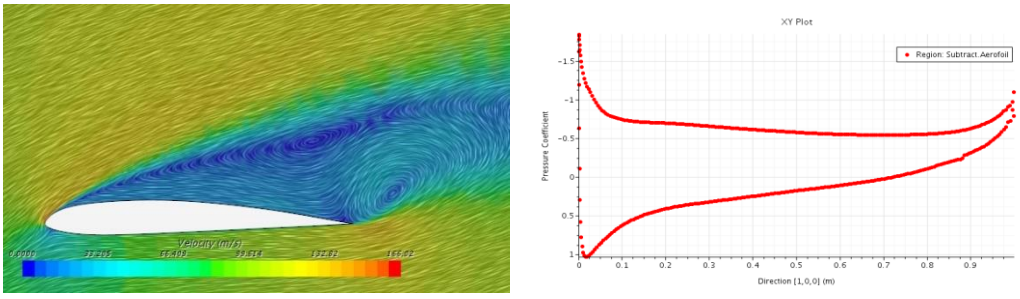

Figure 7: Line integral convolution of the velocity vectors show 2 vortices being shed (left) and a snapshot of the total pressure distribution (right) for DF102-PT simulated at $Re = 300\,900$, M = 0.3 and $\alpha = 18^{\circ}$

Integral coefficients and residuals show periodic behaviour beyond 500 iterations. The residuals have a much larger order of magnitude, with one momentum residual briefly peaking above 1, making it hard to define convergence. The velocity vectors in Figure 7 show large areas of

circulation in the wake. The eddies introduce pressure fluctuations, causing larger fluctuations in C_L compared to C_D, 40% and 10% respectively. This is characteristic of an unsteady wake. Examining the snapshot of the fluctuating C_P distribution, a near constant pressure region extends from 10% to 90% of the chord. This is in line with the large region of separated flow. The pressure peaks again close to the root because of the vortex forming and shedding at the trailing edge.

e. To accurately simulate the flow, how could you further refine the mesh for flows with high incidence angles? (100 words max.)

The flow feature here that affects the performance is the wake. This region is unsteady, containing large gradients and typically turbulent with eddies of various length scales forming and shedding downstream. Wake refinement creates a finer mesh in the direction of the wake, allowing the eddies and gradients to be resolved and better represent the flow physics. The higher curvature also causes higher local Reynolds numbers and a thicker boundary layer, hence the need for a smaller near wall thickness of the prism layer to maintain suitable $y+$ values and thicker total prism layers to encapsulate the thicker boundary layer.

f. Comment on the suitability of the applied *STAR-CCM+* physics models? (125 words max.)

At the low speed and low angle, it is unlikely that most of the flow is turbulent. This is corroborated by the transition point of $\frac{x}{c} > 0.80$ from the XFOIL study conducted at $Re = 100{,}000$. While a higher Re will push the transition point closer to the leading edge due to the increased destabilising effect on the boundary layer, unless a fully turbulent flow is known to exist, the inclusion of a reliable transition model is more appropriate than a fully turbulent model with no transition. The $k - \omega$ SST model is a good choice as it models near-wall regions well, ideal at low angles of attack with little separation. Segregated solvers are also ideal for incompressible, low Mach flows.

STAR-CCM+ vs XFOIL Comparison

1. Comparative Plots (11%)

a. Provide the pressure coefficient profile plot, the lift/drag vs. α plot and the drag polar plot:

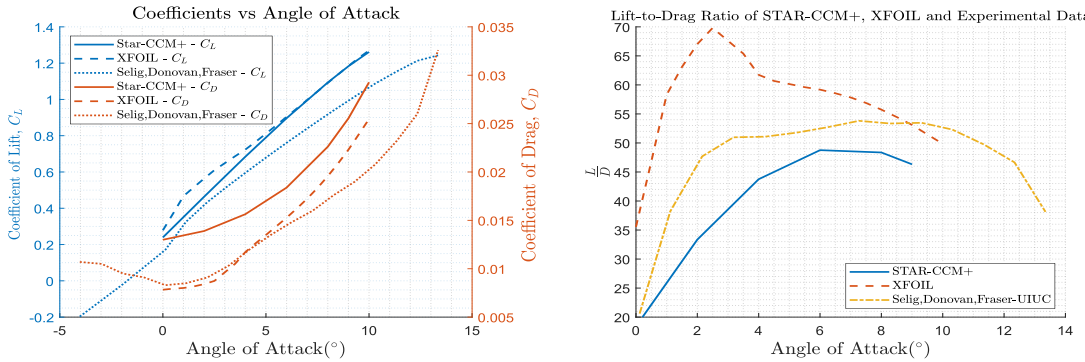

Figure 8: Variation of C_L and C_D with α for DF102-PT from 3 sources(left)
Variation of Lift-to-Drag ratio with α for DF102-PT from 3 sources(right)

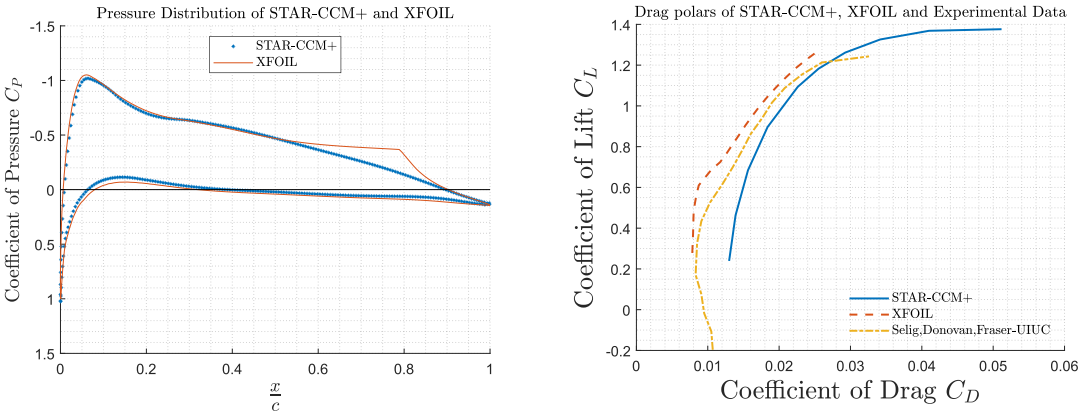

Figure 9: Pressure Distribution at $\alpha = 2^{\circ}$ for STAR-CCM+ and XFOIL for DF102-PT (left)
Drag polars for DF102-PT from 3 sources (right)

2. Comparative Study (15%)

a. Interpret and comment on the Cp results of *STAR-CCM+* and *XFOIL*, including any agreements or differences. (125 words max.)

Both C_P plots are in good agreement. This demonstrates the accuracy of XFOIL for these conditions. The $y+_{max}$ was 0.92, indicating an appropriate mesh to resolve the boundary layer. For most of the chord, STAR-CCM+ predicts a higher pressure on the upper surface and lower pressure on the lower surface, compared to XFOIL. From $0.5 \leq \frac{x}{c} \leq 0.8$, a region of separation, reattachment and finally transition has occurred as discussed under the XFOIL study. The STAR-CCM+ plot lacks this feature as a fully turbulent flow was assumed with no transition model while XFOIL allowed for free transition. Laminar flow results in lower pressure on the upper surface, hence after transition, the agreement of pressure values on the upper surface improves.

b. Identify the differences of the drag polar as well as the lift and drag coefficient results between *STAR-CCM+* and *XFOIL* and the experimental results. What is the reason behind the deviations? (400 words max.)

From Figure 8, STAR-CCM+ overpredicts the C_L and C_D values, followed by XFOIL. At angles 0 to 5. XFOIL has the largest overprediction for C_L followed by STAR-CCM+ for in this range. XFOIL has excellent agreement with experimental data on C_D while STAR-CCM+ overpredicts. A fully turbulent flow is assumed by STAR-CCM hence skin friction will be over predicted. The real flow is transitional at all angles, hence the constant over prediction of C_D by STAR-CCM. A suitable transition model for STAR-CCM+ should see this discrepancy in C_D decrease.

At angles beyond 5, XFOIL has excellent agreement with STAR-CCM+ while both still overpredicting C_L. XFOIL now overpredicts C_D with increasing angles and this is attributed to the inability to model the complex boundary layer interactions occurring at higher angles of attack.

From the right plot in Figure 9Figure 8, the over prediction of C_D discussed leads to the L/D plot for STAR-CCM being the lowest of the 3. Despite the good agreement in C_D for angles below 5, the L/D plot for XFOIL is the highest due to it having the largest overprediction in lift. Referencing Figure 9, STAR-CCM polar is shifted to the right as it produces the largest amount of drag for a given lift and XFOIL shifts to the left, producing more lift for a given drag.

The overprediction of C_L by both solvers is attributed the lack of 3D effects that are present in the test of a finite wing. Both solvers simulate an infinite wing instead. Trailing edge vortices produce a downwash on the suction side of the wing, making it less “efficient” at producing lift for a given angle, hence the discrepancy in C_L despite the similar lift curve slopes. From Table 3, the inability of a fixed mesh to provide a satisfactory y+ value also added to the discrepancy seen in the STAR-CCM values. If the recommendations for mesh refinements in 2e) of this study were implemented, the C_L and C_D from STAR-CCM+ will see closer agreement with the experiments.

c. Which 2D simulation (*XFOIL* or *STAR-CCM+)* do you prefer to use and why? (125 words max.)

STAR-CCM+ offers a wider degree of control over the simulation environment. Larger control is powerful but dependent on the user’s skills as a deeper understanding of the flow physics is needed to accurately set up the simulation and interpret the results. In comparison, XFOIL has fewer commands available. STAR-CCM+ offers a wider variety of field functions, which are customisable to the simulation specific needs. The use of scalar and vector scenes provide visualisation of the flow phenomena. These are useful tools to ascertain if a simulation has been correctly performed and makes “sense”. However, for quick assessment of aerofoil performance within the linear regime and at low, subsonic Mach numbers, the added complexity of STAR-CCM+ becomes unwieldy and XFOIL is the quicker and reliable alternative.

Part B: 3D Wing

AVL

1. Wing geometry (2%)

a. What is the nominal wing area, the tip chord, the root chord, and the x-coordinate of the tip section?

Nominal Wing Area = 0.13935m^2; Tip.C= 0.0762m; Root.C = 0.2286m; x-coord Tip= 0.34016m

2. Drag Polar (5%)

a. Show the *RAE101* drag polar as obtained from *XFOIL*, and your data-fitted polar that *AVL* will operate on. (Disregard the two branches of the polar that are extrapolated beyond the stall angles.)

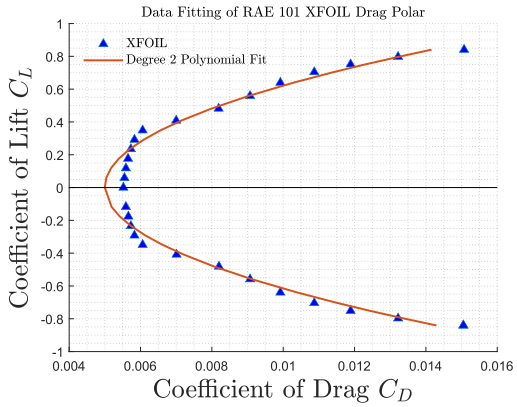

Figure 10: RAE101 drag polar obtained from XFOIL at $Re = 10^6$ and M=0.4 $-7^\circ \leq \alpha \leq 7^\circ$ with a quadratic fit. This fit is poor and can be improved to fit the region of minimum drag better. Due to time constraints this was not performed but using points from this improved fit will provide a more accurate drag polar for AVL

b. Give your chosen parameters of the keyword `CDCL` in *AVL*'s format.

"-0.8407 0.0143 0 0.0050 0.8406 0.0142" as entered in a line in the AVL config file.

3. Vortex Lattice Convergence (12%)

a. Show the vortex-lattice convergence plots using the lift and induced drag coefficients (calculated from Trefftz plane) at a 2° angle of attack with a uniform panel distribution.

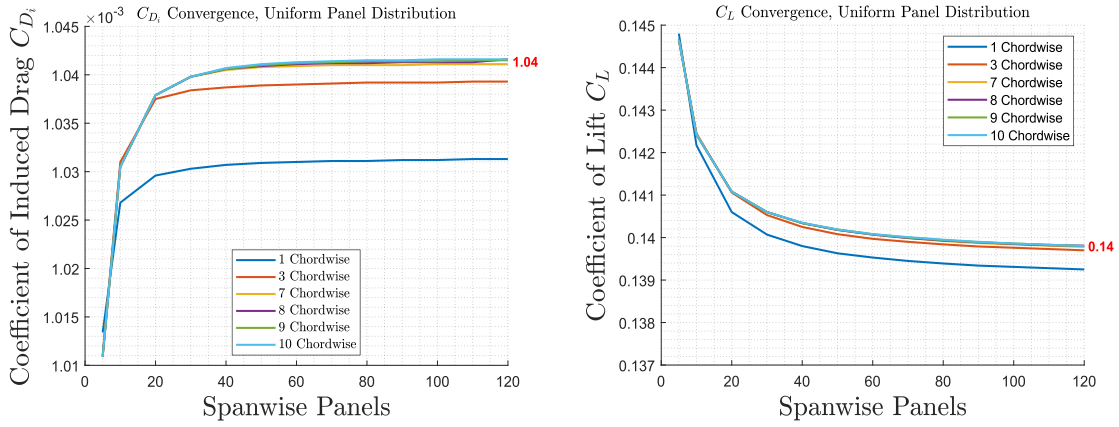

Figure 11: Convergence of C_L and C_{Di} at M=0.4 and $\alpha = 2^\circ$. Uniform span and chordwise distribution

From the convergence study above, 10 chordwise and 100 spanwise vortex-lattices should be used based on a uniform distribution in both directions, a mesh size of $10 \times 100 = 1000$ panels

b. State which vortex-lattice spacing distributions you chose as the most efficient and briefly explain why. (125 words max.)

The cosine distribution will be the most efficient as it concentrates vortex-lattices at spaces that require a finer spacing of vortices due to discontinuities and rapid changes in circulation. In the chordwise direction such distribution places more vortex-lattices at the trailing and leading edges. In the spanwise, more vortex-lattices are found at the wing root and at the tips.

c. Based on the new selected distributions, which number of span and chordwise vortex-lattices will you use for the remaining questions? Make a very brief comment on the comparison of these numbers to those you obtained with the uniform distribution. (50 words max.)

A second convergence study was performed with a cosine distribution and the number of span and chordwise vortex-lattices chosen is 30 and 5 respectively. A reduced mesh size of 150 was required to converge to the same solution. This significantly saves on computational time.

4. Lift Distribution Results (10%)

a. Show, in one plot, the lift distribution and sectional lift coefficients, both from the Trefftz plane and the experimental data.

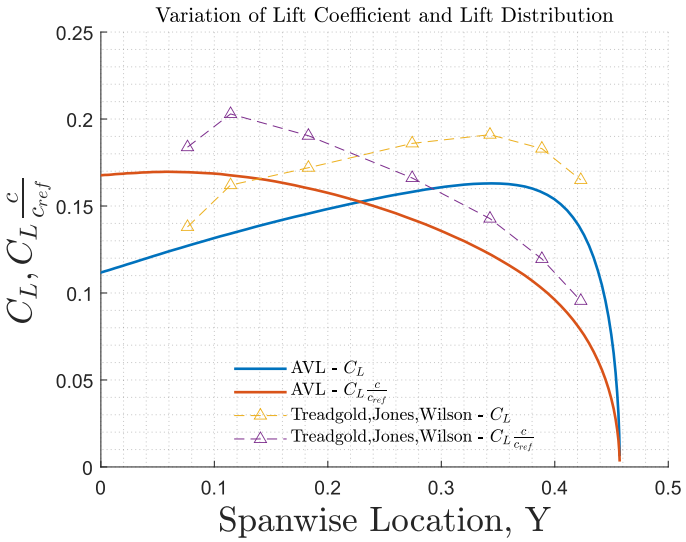

Figure 12: Symmetric Half span lift distribution and sectional lift coefficients for RAE 101 wing from the Trefftz plane and experimental data

b. Briefly discuss the results and comment on how well the calculated and experimental data match and explain any discrepancies. (275 words max.)

The overall trend of the sectional lift coefficient and lift distribution across the span matches the experimental data but under prediction of the values for both variables. Despite the freestream flow exceeding the limits for incompressibility (M0.4>M0.3), AVL was still able to model the behaviour well as it utilised the Subsonic Prandtl-Glauert (PG) compressibility treatment. The PG treatment allows the compressible problem to be treated as an incompressible problem, making it suitable for the vortice-lattice method. The PG model is expected to be valid up to M0.6.

$$M_{\perp} = M\cos(Sweep\ Angle) = 0.32 > 0.3$$

While $M_{\perp}$ (wing perpendicular M) is within the range of validity for the PG model, it still breaks the incompressibility limit hence the underprediction as it does not account for real flow effects. AVL relies on the thin aerofoil theory to perform lift calculations however, the aerofoil section used is RAE101, which has a max thickness to chord ratio of 10% thus it cannot be considered thin. The extra lift contributed from aerofoil thickness is not accounted by AVL, hence lower lift values. The dip in both experimental curves at Y=0.1 is likely due to the fuselage body that was tested. This feature was not included in the AVL study, which modelled a finite swept wing connected at the root. This wing-body interaction likely reduced experimental lift data. The fuselage was probably left out as AVL models the fuselages using slender-body theory and experiences with this theory are limited and not well understood. The lift distribution obtained from AVL is near elliptical, indicating that the geometry has been optimised to provide the minimum induced drag configuration from the wingspan.

5. Determining the maximum lift over drag ratio (5%)

a. Provide the plot showing the lift over drag ratio L/D for the specified range of angles of incidence.

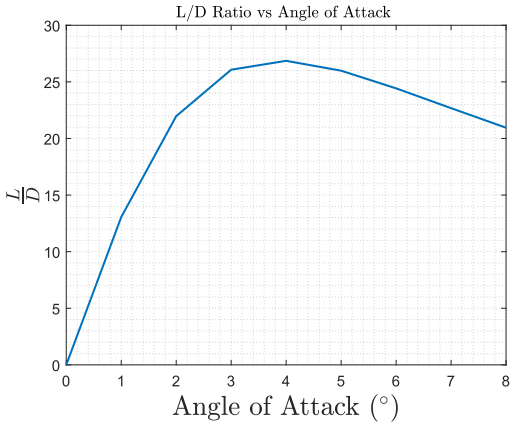

Figure 13: Variation in L/D ratio with angle of incidence for RAE 101. $L/D|_{max}$= 26.9 at $\alpha = 4^{\circ}$

b. What is the optimal angle of incidence for this wing and which L/D ratio can it achieve?

The optimal angle of incidence is approximately 4° with a L/D ratio of 26.9

6. Wing Configuration file (5%)

Refer to Submission Folder

3D *STAR-CCM+*

1. Meshing (12%)

a. Provide the mesh scene image showing the symmetry plane and wing surface mesh.

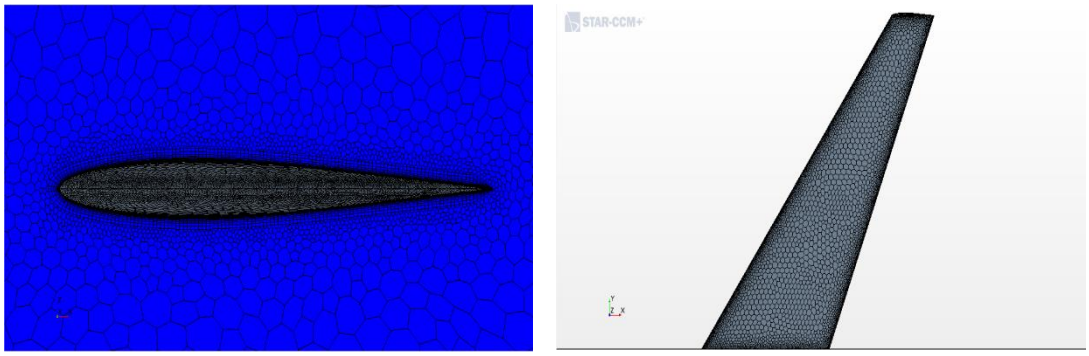

Figure 14: Symmetry plane (left) and wing surface (right) mesh for M=0.4

b. List your mesh parameters and justify your choice – how did you arrive at the values you used? (250 words max.)

The height of the boundary layer must be first be estimated from the equation below:

$$\delta = \frac{0.37x}{Re_x^{1/5}}; \qquad y+ = \frac{\Delta s\, u_\tau}{\nu} \qquad (4)$$

This will be the total height of the prism layers. It is crucial that boundary layer is encapsulated by the prism layers. This requires wall y+ <1. The wall y+ value is related to the distance of the centroid of the first cell, Δs to the boundary, by the equation above, where u_τ and ν are the shear stress velocity and kinematic viscosity respectively. The following two equations were then used to find u_τ and by constraining y+<1, obtain a value for Δs. As this is the centroid position, the thickness of the first prism cell will be $2\Delta s$.

$$C_f = (2\,log(Re) - 0.6)^{-2.3}; \qquad \tau_\omega = \frac{1}{2} C_f\, \rho U_\infty{}^2 \qquad (5)$$

$$Number\ of\ Prism\ Layers = \frac{log\left(\frac{\delta}{2\Delta s}\right)}{log(Expansion\ Ratio)} \quad (6)$$

The number prism layers were found the equation above. A suitable expansion ratio was chosen as 1.3. The right expansion ratio allows the prism layers to grow from the wall to meet the volume mesh smoothly (without sharp jumps in geometry from prism layer to volume cell). This reduces the chances of poor mesh quality. Although an adjusted $2\Delta s$ was obtained, the decision was made to not recalculate the number of prism layers required as doing so would have exceeded the limits set on the total cell count. $2\Delta s_{adjusted}$ still provided a smooth transition from prism layer to volume mesh hence it was deemed to be acceptable.

Table 4: Mesh parameters for subsonic and transonic simulations.

Mach Number	0.4	0.8
Base Size	0.008m	0.008m
Boundary Thickness, δ	0.0049m	0.0049m
First Cell Thickness, $2\Delta s$	$1.92 \times 10^{-5}\ m$	$1.92 \times 10^{-5}\ m$
Prism Layers	22	22
$2\Delta s_{adjusted}$	$1.60 \times 10^{-6}\ m$	$1.60 \times 10^{-6}\ m$
Cell Count ($\times 10^3$)	628	628

c. How did you ensure the y+ target was met? Were there any issues (minor or otherwise) encountered in this task, if so, what was it? Do you expect it to significantly affect the results? (150 words max.)

During the initial simulation, higher than expected values along the discontinuities (y+ > 1). This was expected as the shear velocity used was obtained from approximations of skin friction on a turbulent flat plate. Anomalously large (y+ >>1) where the trailing edge at the root meets the symmetry plane was postulated to be caused by poor mesh quality and was resolved by decreasing the base size. As y+ is directly proportional to Δs, the adjusted value of $2\Delta s$ was obtained by dividing the initial $2\Delta s$ by the max y+, giving the required range of y+.

y+ values affect the result as wall treatment and turbulence models require an appropriate refinement of the mesh encapsulating the boundary layer (prism layers) to resolve the boundary layer variables accurately. At the low angles of attack tested, viscous drag will dominate, and thus inaccurate boundary layer variables will yield inaccurate readings for drag.

2. Physics Settings (5%)

a. What values have you set for flow speed, temperature, pressure, and viscosity:

i. $U_\infty|_{M=0.4} = 141.2\ \mathrm{m/s}$ $\quad U_\infty|_{M=0.8} = 270.1\ \mathrm{m/s}$

ii. $T|_{M=0.4} = 310.1\mathrm{K}$; $\quad T|_{M=0.8} = 283.7\mathrm{K}$

iii. $P|_{M=0.4} = 81{,}640\ \mathrm{Pa}$; $\quad P|_{M=0.8} = 36{,}460\ \mathrm{Pa}$

iv. $\mu|_{M=0.4} = 1.975 \times 10^{-5}\ \mathrm{Pa \cdot s}$; $\quad \mu|_{M=0.8} = 1.844 \times 10^{-5}\ \mathrm{Pa \cdot s}$

b. How did you obtain the values set? (50 words max.)

From experimental stagnation temperature, static temperature is obtained via the isentropic relations, followed by a and freestream velocity, U_∞ Dynamic viscosity is found using Sunderland's Law with constants μ_0, T_0 and S.

$$\mu = \mu_0 \left(\frac{T}{T_0}\right)^{3/2} \frac{T_0 + S}{T + S} \quad (7)$$

Reference Pressure $P|_M$ and Density $\rho|_M$ is obtained by solving the equations for an ideal gas and Reynolds Number.

$$P = \rho R T\ ; \qquad Re = \frac{\rho U_\infty D_{MAC}}{\mu} \quad (8)$$

3. Results (19%)

a. Provide the iteration history of the lift/drag coefficients and residuals plots and write down the obtained converged coefficients:

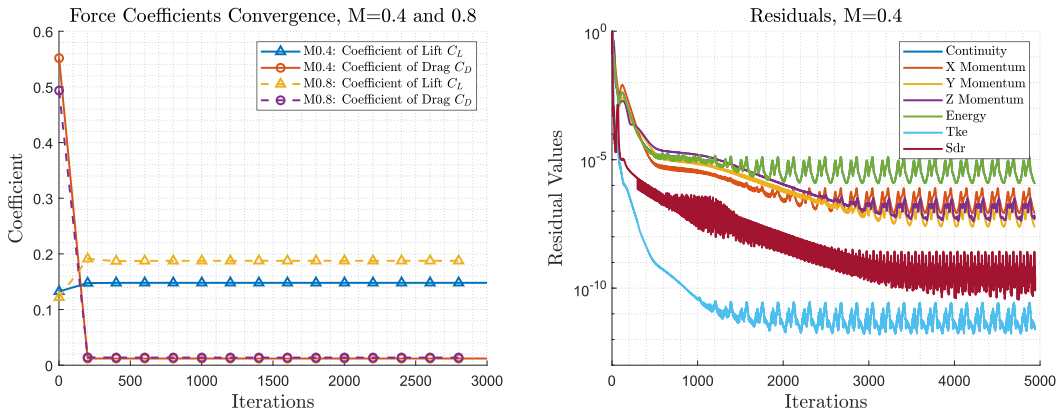

Figure 15: Convergence of the force coefficients for $Re = 10^6$, M0.4 and M0.8 (left) Residuals for the subsonic test case (right)

i. $C_L|_{M=0.4} = 0.1480$; $C_L|_{M=0.8} = 0.1875$

ii. $C_D|_{M=0.4} = 0.0120$; $C_D|_{M=0.8} = 0.0137$

b. Provide the Cp vs. x plots as mentioned in 'PROCESSING INSTRUCTIONS':

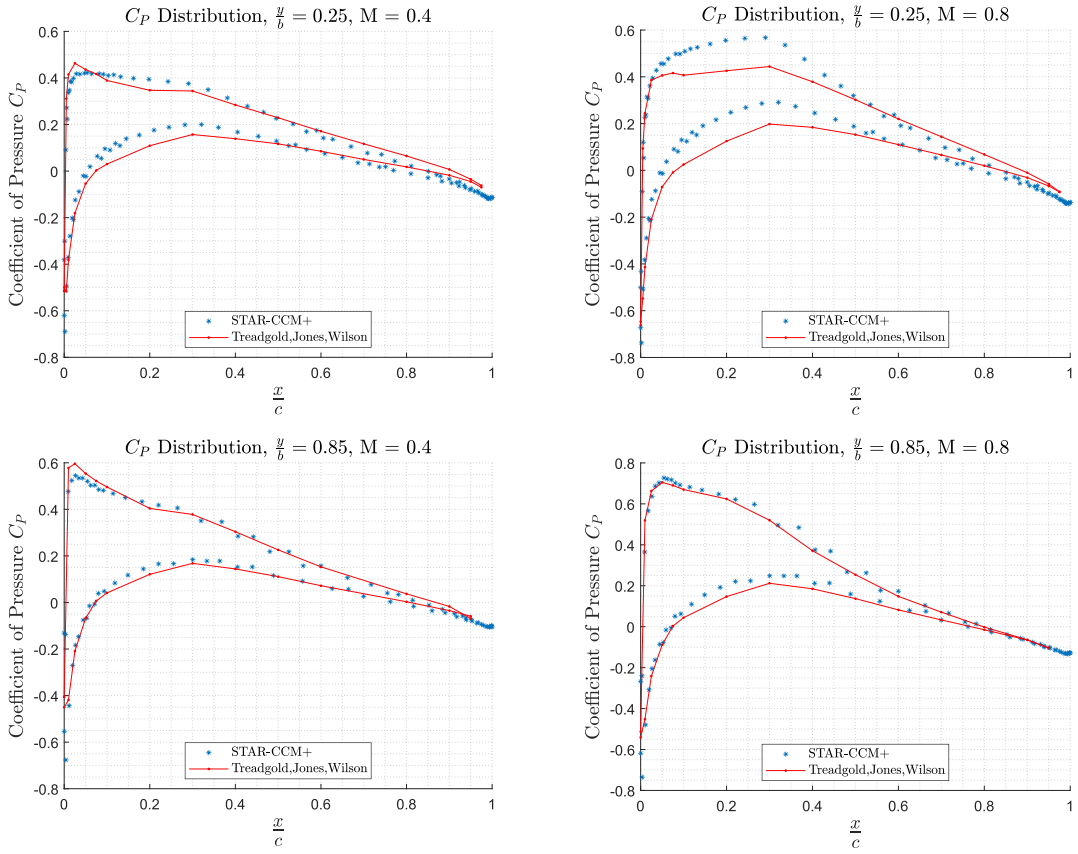

Figure 16: C_P distribution at two spanwise locations for $Re = 10^6$, M0.4 (left) and M0.8 (right)

c. Discuss the Cp vs. x results of *STAR-CCM+* and the experimental data. Interpret any notable differences or agreements. (150 words max.)

Overall STAR-CCM+ is in good agreement with the experimental data. There is a noticeable deviation in the distribution for M0.8. This is attributed to the y+ values being in range. The boundary layer behaviour is thus well modelled by the wall treatment and turbulence models.

For M0.4, the suction peaks are underpredicted by STAR-CCM+. This is due to the fully turbulent model with no transition, whereas the real flow is transitional.

At y/b=0.25 and M0.4, a region of constant pressure is observed from 0.025 < x/c < 0.125 before decreasing, indicating a separation bubble. This is characteristic of leading-edge stall.

For M0.8 at y/b=0.25, the suction peaks are overpredicted by STAR-CCM+. A shock has likely occurred at x/c ≈ 0.30. Current mesh settings are not suited for shock simulation led to an overestimation of the pressure rise, yielding the higher suction peak observed as compared to the experimental data.

4. Summary Report (10%**)**

Refer to Submission Folder

STAR-CCM+ vs AVL Comparison

1. Comparative Plots (4%**)**

a. Provide the comparative pressure coefficient deltas (dCp) plot from the two subsonic simulations (*XFOIL* and *STAR-CCM+*) with the experimental data:

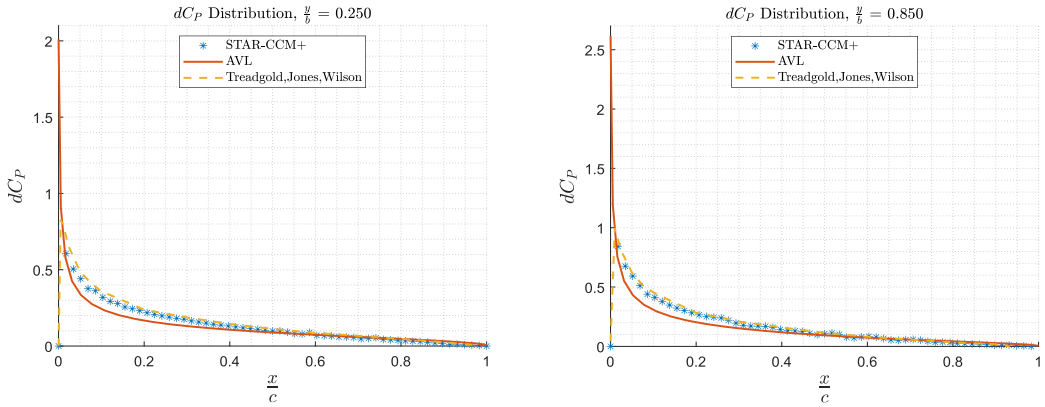

Figure 17: dC_P distribution at two spanwise locations for $Re = 10^6$, M0.4 and M0.8.

2. Comparative Study (11%**)**

a. Interpret the dCp results of the experimental data, *STAR-CCM+* and *AVL* as well as any differences between the 3 datasets. (175 words max.)

The overall shape of the dC_P distribution is well predicted by both solvers. dC_P at the leading and trailing edge must be zero as the coordinates are identical for both upper and lower surfaces. AVL was unable to predict this at the leading edge, highlighting the difficulty it faces in modelling regions of high curvature.

In both cases, dC_P was underpredicted from the leading edge to approximately 70% of the chord but STAR-CCM+ outperformed AVL in predicting the shape of the curve. The physical flow is viscid and STAR-CCM+ has wall treatment and turbulence models to resolve the boundary layer variables, providing more accurate readings than AVL's inviscid solution.

While not clearly visible, from 70% of the chord to the trailing edge, AVL begins to overpredict dC_P closer to the trailing edge. Both STAR-CCM+ and the experimental values dip below AVL's prediction at approximately the same locations. This deviation is due to AVL's inability to predict flow separation, which results in the halting of pressure drop across the chord as the flow detaches.

b. List a total of at least four advantages and disadvantages of *STAR-CCM+* over *AVL*. Which software would you use when designing a wing and why? (200 words max.)

1. STAR-CCM+ can model viscous flow, while AVL cannot.
2. STAR-CCM+ can model supersonic and transonic effects with the appropriate settings, providing a wider range of test conditions, increasing usability
3. STAR-CCM+ can model unsteady flow when given appropriate inputs while AVL cannot, increasing the range of flows available for testing.
4. STAR-CCM+ can work with thick aerofoils, while AVL's suffers in such a configuration due to the large curvatures.
5. AVL allows for rapid turnaround times during early prototyping (e.g. Selecting the aerofoil sections and their placements along the wing)
6. AVL is a free and readily available software while STAR-CCM+ requires a subscription to a commercial license
7. AVL provides reasonable predictions for integral values (C_L, C_D, C_{D_i}) under inviscid and incompressible conditions and some small ranges of compressible conditions for its simplicity to in setup compared to STAR-CCM+
8. STAR-CCM+ requires more training and knowledge to setup correctly. AVL has substantially lesser variables and makes it an easier simulation software to learn.

AVL is used during the early design phase such as for selecting aerofoils, sweep and other related design decisions. before transitioning to STAR-CCM+ for in-depth aerodynamic analysis